Dielectric Relaxation Spectroscopy

C.M. Roland

(December 17, 2014)

Introduction

Impedance spectroscopy and dielectric relaxation measurements yield the same information; however, their purpose and analysis methods differ. Impedance spectroscopy is typically used to probe electrochemical processes, while dielectric relaxation data, almost invariably expressed in the complex permittivity representation, provide information on dynamical processes, typically the rate of molecular or polymer chain reorientation. Moreover, the features of interest in an impedance measurement, such as the transport and adsorption of charges, are an unwanted contribution to dielectric relaxation spectra, and thus are either ignored or removed from the latter. (Occasionally, the impedance function representation is used to eliminate interferences with relaxation measurements.) Since the objective of dielectric spectroscopy is to characterize the dynamics, models of molecular motion are the basis for interpretation; equivalent circuits, prominent in impedance spectroscopy studies, are not employed to analyze relaxation spectra. However, since relaxation spectra can be described formally as a distribution of exponential relaxation processes [1,2], an equivalent circuit diagram can be constructed (**Figure 1** [3]). Such a description is phenomenological (a mathematical convenience), and its underlying premise, that the observed peak shape reflects a distribution of exponential decays, is problematic [4,5]. Table 1 summarizes the distinct aspects of impedance and dielectric relaxation spectroscopies.

Dielectric relaxation.

The use of dielectric spectroscopy to probe the motion of molecules requires the latter to have a nonzero dipole moment, μ. However, with modern instrumentation capable of attofarad resolution, this is not a restrictive requirement. Even conventional dielectric bridges can measure polymers with very small dipole moments ($\mu<0.1$ D); for example, atactic polypropylene, which has a dielectric strength less than 0.01 [6,7]. In the usual relaxation measurement, a weak electric field is applied, with the linear response regime defined by two (equivalent) conditions:

(i) The dielectric permittivity does not vary with the electric field, E; this means that the polarization is proportional to E

$$P = \left(\varepsilon * -1 \right) \varepsilon_0 E \tag{1}$$

where $\varepsilon*$ is the complex dielectric permittivity of the material and ε_0 the dielectric permittivity of vacuum (=8.854 pF/m).

(ii) The polarization energy, associated with dipole orientation, is less than the thermal energy; i.e., μE << kT. This means there is no net polarization, as orientation of the dipoles is overcome by thermal agitation, and the sample remains isotropic.

Since the motions prevailing at equilibrium enable the molecular dipoles to remain unoriented on average, the measured time-dependent fluctuations of the polarization correspond to the equilibrium dynamics. For small molecules (simple liquids) dielectric relaxation spectroscopy probes the molecular reorientations. For most polymers the dipole moment is transverse to the chain, so that the dielectric experiment probes the local segmental dynamics. For those few polymers having a dipole moment component parallel to the backbone (which means their repeat unit structure lacks a symmetric center), dielectric relaxation can measure more global dynamics, as discussed below. Expressing eq.(1) for the dynamics gives

$$P(t) = P_\infty + \varepsilon_0 \int_{-\infty}^{t} \varepsilon(t-t') \frac{dE(t')}{dt'} dt' \tag{2}$$

in which P_∞ accounts for induced polarization (e.g., distortion of the electron cloud), and the second term describes the orientation polarization. The usual experiment applies a time-dependent electric field, with the complex permittivity obtained as

$$\varepsilon^*(\omega) = \varepsilon'(\omega) - i\varepsilon''(\omega) = \varepsilon_\infty - \int_0^\infty \frac{d\varepsilon(t)}{dt} \exp(-i\omega t) dt \tag{3}$$

The relationship to the impedance is

$$\varepsilon^*(\omega) = \frac{1}{i\omega Z^*(\omega) C_0} \tag{4}$$

where $\underline{C_0}$ is the vacuum capacitance. In eq.(3) ε_∞ is the constant value of the dielectric permittivity exhibited by materials at sufficiently high frequencies.

The structural relaxation peak (α-process) of liquids and polymers is invariably broader than the Debye function (for which the peak has a width at the half intensity points of 1.14 decades)

$$\varepsilon^*(\omega) = \varepsilon_\infty + \frac{\Delta\varepsilon}{1 + i\omega\tau_D} \tag{5}$$

where τ_D the Debye relaxation time, and $\Delta\varepsilon$ is the dielectric strength (= ε_s - ε_∞ where ε_s is the static or low frequency permittivity). Structural relaxation spectra are usually fit to either the Havriliak-Negami (H-N) equation [3]

$$\varepsilon*(\omega) = \Delta\varepsilon\left[1 + (\mathrm{i}\omega\tau_{\mathrm{HN}})^a\right]^{-b} \tag{6}$$

where τ_{HN}, a, and b are constants, or the Kohlrausch-Williams-Watts (KWW) function [3]

$$\varepsilon*(\omega) = \Delta\varepsilon\,\hat{L}_{i\omega}\left[-\frac{d\varphi(t)}{dt}\right] \tag{7}$$

$$\varphi(t) = \exp\left[-\left(t/\tau_K\right)^{\beta_K}\right] \tag{8}$$

with τ_K and β_K constants, and $\hat{L}_{i\omega}$ denotes the Laplace transform. Eq. (6) is empirical, its popularity deriving from the ability to fit experimental $\varepsilon''(\omega)$ peaks. Eq. (8), which has one less adjustable parameter than the H-N equation, can be arrived at in various ways: from models based on free volume [8], hierarchal constraints [9], defect diffusion [10], defect distances [11], random free energy [12], intermolecular cooperativity [13,14], or molecular weight polydispersity [15]. The KWW function can also be obtained by employing a particular distribution of exponential decay functions [1,2], illustrated by the equivalent circuit in Fig. 1. Secondary relaxations, which fall at higher frequencies, can be described by eq.(6) or the symmetric Cole-Cole function [3]

$$\varepsilon*(\omega) = \frac{\Delta\varepsilon}{1 + (\mathrm{i}\,\omega\tau_{CC})^{1-\gamma}} \tag{9}$$

where γ and τ_{cc} are constants. Eq. (9) corresponds to the H-N function with $b=1$, and reduces to the Debye function for $\gamma=0$. The peak in the dielectric loss spectrum occurs at a frequency corresponding to that of the underlying molecular motions (e.g., rotations of small molecules or the local segmental dynamics of polymers for their α-relaxation peak). Thus, the inverse of the α-peak frequency defines a model-independent relaxation time, τ_α. Reflecting the stretching of the spectrum toward longer frequencies, $\tau_\alpha > \tau_K$, while the relative magnitudes of τ_K and τ_{HN} depend on the shape parameters, a, b, and β_K.

Figure 2 shows the dielectric relaxation spectrum of polymethylmethacrylate (PMMA), which has an unusually prominent secondary relaxation. If the latter is well separated from the α-peak, the two dispersions can be fit with the assumption that the processes are additive in the frequency domain. If the respective τ are close, this assumption breaks down, and an equation due to Williams [16] is used

$$\varepsilon(t) = f_\alpha\varepsilon_\alpha(t) + (1 - f_\alpha)\varepsilon_\beta(t) \tag{10}$$

Eq. (10) assumes the two relaxations are independent, except that the β process takes place in an environment that is rearranging on the timescale of the α-process. The fits of eqs.(6) and (7)-(8), using

eq. (10), to the PMMA dielectric constant and loss spectra are shown in the Fig. 2. Note that the dielectric loss exhibits power-law behavior at low frequencies, a consequence of mobile ions; this dc-conductivity is discussed below.

The main features of the dielectric spectra of polymers are the α-relaxation peak due to the local segmental dynamics and various higher frequency, secondary relaxations due to restricted torsional motions of the chain and any side group dynamics. However, polymers having a dipole moment parallel to the chain contour (e.g., 1,4-polyisoprene, polypropylene glycol (PPG), polylactide) exhibit a so-called normal mode peak due to fluctuations of the chain end-to-end vector [17]. Spectra are shown in **Figure 3** for PPG and polyoxybutylene (POB) [18], both polymers having dielectrically active normal modes. Sometimes referred to as the global or terminal relaxation, the normal mode peak falls at lower frequencies than the local segmental dispersion, by an amount nonlinear in the polymer molecular weight [5]. At high temperatures the two relaxation processes have equivalent *T*-dependences, whereas at temperatures approaching the glass transition, the normal mode relaxation time is less sensitive to temperature than the more local α-process [19].

Ion conductivity. Liquids and polymers invariably contain mobile ions, often electrolytic impurities, whose diffusion gives rise to dc-conductivity, σ_{dc} (see Fig. 2). In a material that is inherently conducting, σ_{dc} may correspond to translocation of intrinsic ions across sites on a polymer chain, such as protons along hydrogen bonds. This conduction is distinct from the higher frequency ac conductivity, which in addition to ion diffusion can arise from nonrelaxing, subdiffusive processes, such as local excursions and vibrations of ions within a cage of the host molecules. Whereas a common purpose of impedance spectroscopy is to characterize ion diffusion, for relaxation studies σ_{dc} is usually unwanted because it can mask the relaxation peaks in the loss spectrum. The Nernst equation relates the dc-conductivity to the concentration of ions, *c*, having charge *q* [20]

$$\sigma_{dc} = c\,q^2 D / k_B T \tag{11}$$

where *D* is the ion diffusion constant and k_B the Boltzmann constant. For a frequency dependent diffusion constant, *D*(ω)*, the conductivity is complex and yields a term in the permittivity

$$\varepsilon^*(\omega) = \frac{\sigma^*(\omega)}{\mathrm{i}\,\omega \varepsilon_0} \tag{12}$$

The usual power-law behavior gives

$$\varepsilon^*(\omega) = \frac{\sigma_{dc}}{\varepsilon_0 (\mathrm{i}\omega)^j} \tag{13}$$

with j a constant ($\leq$ 1), equal to unity for free conduction of electrons or ions. This conductivity contribution to the dielectric loss can be described by

$$\varepsilon_{dc}^{''}(\omega) = \frac{\sigma_{dc}}{\varepsilon_0 \omega^j} \tag{14}$$

Provided there is some separation from the relaxation peaks, eq.(14) can be included in fitting spectra to account for the conductivity.

Ionic conductivity is coupled to reorientational relaxation, since motion of the host molecules or segments provides diffusive pathways. This leads to a relation between ion conductivity and the α-relaxation time [21]

$$\sigma_{dc} \tau_\alpha^j = const \tag{15}$$

Eq. (15) is an empirical variation of the Debye-Stokes-Einstein (DSE) equation [22],

$$\frac{\sigma_{dc} \tau_\alpha T}{c} = const. \tag{16}$$

Generally, c and T change little over the range of dielectric measurements, so that σ_{DC} is plotted versus τ_α on double logarithmic scales, to yield a power-law having a slope equal to $-j$. Results are shown in **Figure 4** for propylene glycol monomer, dimer, and trimer. The exponent (j= 0.84$\pm$0.02) is the same for the three liquids, although the magnitude of the ion conductivity decreases with increasing molecular weight.

The conductivity behavior described by the fractional DSE eq.(15) can have two origins. Any change in the ion population due to polyelectrolytic dissociation or the formation of ion pairs is usually neglected in analysis of data (that is, c is assumed constant). And since the effect of temperature and pressure on ion population is usually very different from their influence on ion mobility, the result can be deviations from proportionality of σ_{dc} to the inverse relaxation time. The other cause of departures from eq.(16) is more general: As temperature is reduced below approximately 1.2T_g, a reduction in the coupling between translational and rotational dynamics is observed [23]. This is manifested in the T-dependence of translational diffusion becoming weaker than that of the viscosity or the rotational dynamics, causing a violation of the DSE equation (**Figure 5** [5]). The mechanism underlying this decoupling is not well understood.

Although dc-conductivity sometimes interferes with characterization of molecular relaxation, the dependence of ion diffusion on the α-dynamics can be exploited to obtain information about structural relaxation of a glass. By definition, the glassy state corresponds to conditions for which

molecular diffusion and rotation (or local segmental motion of a polymer) transpire more slowly than the observable time scale; that is, their loss peaks are at frequencies lower than measured by dielectric spectroscopy (< 10^{-4} Hz). However, the cessation of these motions retards, but does not preclude, ion diffusion. Thus, below the glass transition ion conduction continues, although the sensitivity of σ_{dc} to temperature (i.e., the activation energy) and to pressure (the activation volume) both decrease. The reduced activation energy below T_g is illustrated in **Figure 6** in a plot of the conductivity relaxation time (defined below) for an ionic liquid versus temperature [24]. Physical aging (very gradual densification) of the glass slows the ion diffusion; the time constant describing this effect corresponds to a structural relaxation time, which is too large for direct measurement (below T_g τ_α in Fig. 6 exceeds 8 hours).

An obvious method to minimize the conductivity contribution to the spectrum is to reduce the ion concentration. This can be done by successive dissolution-precipitation of the polymer, or by application of an electric field to the sample *in situ* to cause accumulation of the ions at the electrode interfaces for subsequent removal [25]. From the Kramers-Kronig relation for the case of *j*=1 (eq.(16))

$$\varepsilon'(\omega) = \varepsilon_\infty + \frac{2}{\pi} \int_0^\infty \varepsilon''(\omega_0) \frac{\omega_0}{\omega_0^2 - \omega^2} d\omega_0 \tag{17}$$

$$\varepsilon''(\omega) = \frac{\sigma_{dc}}{\varepsilon_0 \omega} + \frac{2}{\pi} \int_0^\infty \varepsilon'(\omega_0) \frac{\omega_0}{\omega_0^2 - \omega^2} d\omega_0 \tag{18}$$

it is seen that the dc-conductivity makes no contribution to the real part of the permittivity; thus, the measured $\varepsilon'(\omega)$ can be converted via eq. (18) to a dielectric loss spectrum without interference from σ_{dc}. This is illustrated in **Figure 7** [26], showing the measured and calculated dielectric loss for a liquid with a substantial conductivity.

For broad relaxation peaks an approximation to the Kramers-Kronig formula can be used [26]

$$\varepsilon''(\omega) \approx -\frac{\pi}{2} \frac{\partial \varepsilon'(\omega)}{\partial \ln \omega} \tag{19}$$

The dc-conductivity is absent from this calculated dielectric loss. An example of the application of eq. (19) is included in Fig. 7; it can be seen that the α-peak in the derivative spectrum is artificially narrower than in the directly measured $\varepsilon''(\omega)$, although the frequencies of the maxima, and thus the τ_α, coincide. This derivative analysis can also be employed to shift the effect of electrode polarization toward lower frequencies, away from the main relaxation [27]. Electrode polarization refers to blocking of charge exchange at the sample-electrode interface, due to the existence of a potential barrier. Mainly arising in more conductive systems, electrode polarization causes the measured dielectric constant at low frequency to be much larger (in the range $10^2 - 10^6$) than the actual value for the sample.

Dielectric modulus. The dielectric function $\varepsilon^*(\omega)$ is a compliance, the ratio of the electric displacement to the field. Analogous to the mechanical compliance and modulus, a dielectric modulus ("reciprocal permittivity") can be defined

$$M^*(\omega) = 1/\varepsilon^*(\omega)$$

$$M'(\omega) = \frac{\varepsilon'}{\varepsilon'^2 + \varepsilon''^2} \tag{20}$$

$$M''(\omega) = \frac{\varepsilon''}{\varepsilon'^2 + \varepsilon''^2}$$

The permittivity describes the polarization at constant field, and $M^*(\omega)$ the polarization at constant charge. Of course, the modulus representation contains no information not present in the dielectric permittivity; however, the dc-conductivity is manifested in the imaginary component, $M''(\omega)$, as a peak, and the α-relaxation is shifted to higher frequency; thus, the latter is more separated from σ_{dc} than in the permittivity representation. The amount of this shift of the α-peak depends on the dielectric strength of the relaxation; for a Debye process (eq.(5)), $\tau_{\alpha,\varepsilon''} = \frac{\varepsilon_s}{\varepsilon_\infty}\tau_{\alpha,M''}$. This effect and the presence of a conductivity peak in $M''(\omega)$ are shown in **Figure 8**.

The conductivity relaxation time, τ_σ, is defined as the inverse of the frequency of the maximum of the $M''(\omega)$ conductivity peak. This relaxation time differs from the microscopic correlation time, τ_{ion}, describing ion movement (e.g., hopping). From a model of random movement of ions in a disordered medium, a relation can be obtained between the two quantities [28]

$$\tau_{ion}/\tau_\sigma = \frac{cq^2r^2}{6k_BT\varepsilon_0\varepsilon_\infty} \tag{21}$$

where r is the mean hopping displacement of the ions.

Use of impedance function in dielectric relaxation experiments. Dielectric relaxation measurements to determine the dynamics of polymers and liquids analyze the permittivity, ignoring the impedance. However, when measurements are extended to high frequencies (which for a typical dielectric relaxation experiment is defined as frequencies beyond *ca.* 10^6 Hz), the complex impedance may be utilized to remove the effects of the resistance and inductance of electrical cables used to connect the sample electrodes to the analyzer. The relevant equation for the resistance R is

$$\lim_{\omega \to \infty} z'(\omega) = R \tag{22}$$

and for the inductance L (resistance due to current changes in the cable)

$$z''(\omega) = \frac{d}{\omega} - \omega L \tag{23}$$

where d a constant. The measured impedance functions are then corrected to yield spectra free from these effects of the cables

$$z'_{corr}(\omega) = z'(\omega) - R \tag{24}$$

and

$$z''_{corr}(\omega) = \omega L z''(\omega) \tag{25}$$

In turn, the permittivity is calculated from the corrected impedances using eq.(4).

To apply eqs.(22) and (23) requires dielectric measurements that are free from relaxation peaks; i.e., any capacitance changes due to the sample. This can be done by measurements at temperatures well below T_g, as illustrated in **Figure 9** for a crosslinked polyvinylethylene (PVE). The fit to the real and imaginary impedance functions yields respectively R and L for the cable assembly. Eqs. (24) and (25) are used to calculate the corrected impedance functions, from which the permittivity is obtained. **Figure 10** illustrates this method to remove the interference from the cables in measurements on the PVE network, enabling determination of the actual material response [29]. Because of the low polarity of PVE, cable contributions become apparent at relatively low frequencies, *ca.* 2 kHz. More typically, corrections for cable effects are required only for measurements beyond *ca.* 10^6 Hz.

Another use of the impedance function in dielectric spectroscopy is to remove the effects of electrode polarization; that is, charge build-up under low frequency fields at the electrode-sample interface. This phenomenon is an example of the Maxwell-Wagner-Sillars (MWS) effect, which is a general term for polarization, including at an external electrode or at internal boundary layers within an inhomogeneous sample. For the case of an insulating layer covering the electrode, the layer and sample impedances are in series, with the measured impedance equal to the sum of the values for the sample, z_{sam}, and layer, z_{ins}

$$z^*_{meas} = z^*_{sam} + z^*_{ins} \tag{26}$$

From eq.(4)

$$\varepsilon^*_{meas} = \frac{(l_{sam} + l_{ins})\, \varepsilon^*_{sam}\, \varepsilon^*_{ins}}{l_{ins}\varepsilon^*_{sam} + l_{sam}\,\varepsilon^*_{ins}} \tag{27}$$

in which l_{sam} and l_{ins} represent the respective thicknesses of the sample and insulating layers. If the sample has significant conductivity, it will give rise to a peak due to the interfacial polarization at a frequency, f_{MWS}, given by

$$f_{MWS} = \frac{\sigma_{sam}}{2\pi\varepsilon_0 \left(\varepsilon'_{sam} + \frac{l_{sam}}{l_{ins}} \varepsilon'_{ins} \right)} \qquad (28)$$

Electrode polarization can be exploited to separate the contributions of ion concentration and ion mobility to the conductivity [30], although in most relaxation measurements it is an unwanted artifact.

To suppress dc-conductivity in a dielectric loss spectrum, use is sometimes made of a "blocking electrode", which refers to an insulator film placed between the sample and one of the electrodes. Although this method removes the prominent manifestation of σ_{dc} in the response, the steep rise in $\varepsilon''(\omega)$ at lower frequencies (eq.(14)), it does not eliminate the effect of conductivity on the relaxation spectrum. This is shown in **Figure 11** in the dielectric spectrum of xylitol. Introduction of an insulating film causes the conductivity contribution to appear as a loss peak that still masks features of the spectrum in that frequency range.

Dielectric discontinuities within a sample can also give rise to spurious MWS peaks. **Figure 12** shows spectra for glycerol [31], in which at frequencies lower than the α-process there is a strong σ_{dc} contribution, manifested as a power-law in $\varepsilon''(\omega)$ and a rise at lower frequencies in $\varepsilon'(\omega)$ due to electrode polarization. Using the derivative of the real part to obtain the loss spectrum *sans* σ_{dc} reveals a weak MWS peak. The latter can be identified, *inter alia*, by its occurrence at frequencies for which $\varepsilon' \sim \varepsilon''$ [32]. Teflon and other polymeric insulators are also commonly used in the form of an annular ring to contain liquid samples or as a spacer (ring or fibers) to maintain a constant sample thickness. Since the insulators have a finite capacitance, their presence in parallel with the sample can cause a background loss that is additive in the permittivity. This can alter $\Delta\varepsilon$ and shift the frequency of the peaks in the spectrum; typically these errors become significant when the area of the spacer is more than about 0.1% of the sample area [33].

Summary. Impedance spectroscopy and dielectric relaxation measurements employ similar instrumentation, but are used for different purposes. In dielectric spectroscopy the usual objective is determination of the dipole reorientation dynamics that underlies, for example, structural relaxation of liquids and polymers. Contributions to the spectra from dc-conductivity interfere with the measurement of relaxation peaks. This means that the spectral features that comprise the main interest of impedance spectroscopic experiments (e.g., bulk ion conduction, grain boundary and electrode/sample interfacial resistances) must be eliminated in relaxation studies. In this chapter the basics of dipole relaxation

measurements have been outlined, along with a summary of methods used to remove conductivity effects from the spectra.

References

[1] C.P. Lindsey and G.D. Patterson [1980] Detailed comparison of the William-Watts and Cole-Davidson functions, *J. Chem. Phys.* **73**, 3348-3357.

[2] M.N. Berberan-Santos, E.N. Bodunov, and B. Valeur [2005] Mathematical functions for the analysis of luminescence decays with underlying distributions 1. Kohlrausch decay function (stretched exponential), *Chem. Phys.* **315**, 171-182.

[3] *Broadband Dielectric Spectroscopy* [2003] F. Kremer and A. Schonhals (eds.) Springer-Verlag, Berlin.

[4] R. Richert [1994]Homogeneous dispersion of dielectric responses in a simple glass. , *J. Non-Cryst. Sol.* **172-174**, 209-213.

[5] C.M. Roland [2011] *Viscoelastic Behavior of Rubbery Materials*, Oxford Univ. Press, Oxford.

[6] R.N. Work, R.D. McCammon, and R.G. Saba [1964] Effective Dipole Moment of Polypropylene, *J. Chem. Phys.* **41**, 2950.

[7] K. Kessairi, S. Napolitano, S. Capaccioli, P. Rolla, and M. Wubbenhorst [2007] Molecular dynamics of atactic poly(propylene) investigated by broadband dielectric spectroscopy, *Macromolecules* **40**, 1786-1788.

[8] M.H. Cohen and G.S. Grest [1981] Dispersion of relaxation rates in dense liquids and glasses, *Phys. Rev. B* **24**, 4091-4094.

[9] R.G. Palmer, D.L. Stein, E. Abrahams and P.W. Anderson [1984] Models of hierarchically constrained dynamics for glassy relaxation,*Phys. Rev. Lett.* **53**, 958-961.

[10] J.T. Bendler and M.F. Shlesinger [1985] Derivation of the Kohlrausch-Williams-Watts decay law from activation-energy dispersion, *Macromolecules* **18**, 591-592.

[11] J. Klafter and A. Blumen [1985] Models for dynamically controlled relaxation, *Chem. Phys. Lett.* **119**, 377-382.

[12] C. DeDominicis, H. Orland, and F. Lainee [1985] Stretched exponential relaxation in systems with random free-energies, *J. Physq. Lett.* **46**, L463-L466.

[13] K.L. Ngai, R.W. Rendell, A.K. Rajagopal, and S. Teitler [1986] Three coupled relations for relaxations in complex systems, *Ann. NY Acad. Sci.* **484**, 150-184.

[14] M.M. Kubat, P. Riha, R.W. Rychwalski, and S. Uggla [1999] A Kohlrausch type equation based on a simplified cooperative model, *Mech. Time Dep. Matl.* **3**, 31-47 (1999).

[15] P.-G. de Gennes [2002] Relaxation anomalies in linear polymer melts, *Macromolecules* **35**, 3785-3786.

[16] G. Williams [1979] Molecular aspects of multiple dielectric relaxation processes in solid polymers, *Adv. Polym. Sci.* **33**, 59-92.

[17] K. Adachi and T. Kotaka [1993] Dielectric normal mode relaxation, *Prog. Polym. Sci.* **18**, 585-622.

[18] R. Casalini and C.M. Roland [2005] Temperature and density effects on the local segmental and Global chain dynamics of poly(oxybutylene), *Macromolecules* **38**, 1779-1788.

[19] C.M. Roland, K.L. Ngai, P.G. Santangelo, X.H. Qiu, M.D. Ediger, and D.J. Plazek [2001] Temperature dependence of segmental and terminal relaxation in atactic polypropylene, *Macromolecules* **34**, 6159-6160.

[20] G.P. Johari and O. Andersson [2006] On the nonlinear variation of dc conductivity with dielectric relaxation time, *J. Chem. Phys.* **125**, 124501.

[21] S. Corezzi, E. Campani, P. A. Rolla, S. Capaccioli, and D. Fioretto [1999] Change in dynamics of supercooled systems revealed by dielectric spectroscopy, *J. Chem. Phys.* **111**, 9343-9351 (1999).

[22] F. Stickel, E. W. Fischer, and R. Richert [1996] Dynamics of glass-forming liquids. II. Detailed comparison of dielectric relaxation, dc-conductivity, and viscosity data *J. Chem. Phys.* **104**, 2043-2055.

[23] M.D. Ediger [2000] Spatially heterogeneous dynamics in supercooled liquids. *Annu. Rev. Phys. Chem.* **51**, 99–128.

[24] Z. Wojnarowska, C.M. Roland, K. Kolodziejczyk, A. Swiety-Pospiech, K. Grzybowska, and M. Paluch [2012] Quantifying the structural dynamics of pharmaceuticals in the glassy state, *J. Phys. Chem. Lett.* 3, 1238-1241.

[25] C. Gainaru, R. Bohmer, and G. Williams [2010] Ion sweeping in conducting dielectric materials, *Eur. Phys. J.* **75**, 209-216.

[26] M. Wubbenhorst and J. van Turnhout [2002] Analysis of complex dielectric spectra. I. One-dimensional derivative techniques and three-dimensional modelling, *J. Non-Cryst. Sol.* **305**, 40-49.

[27] M.L. Jimenez, F.J. Arroyo, J. van Turnhout, and A.V. Delgado [2002] Analysis of the dielectric permittivity of suspensions by means of the logarithmic derivative of its real part, *J. Coll. Interface Sci.* **249**, 327-335.

[28] K.L. Ngai and C. Leon [1999] Relating macroscopic electrical relaxation to microscopic movements of the ions in ionically conducting materials by theory and experiment, *Phys. Rev. B* **60**, 9396-9405.

[29] R.Casalini and C.M. Roland [2010] Effect of crosslinking on the secondary relaxation in polyvinylethylene, *J. Polym. Sci. Polym. Phys. Ed.* **48**, 582-587.

[30] R.J. Klein, S. Zhang, S. Dou, B.H. Jones, R.H. Colby, and J. Runt [2006] Modeling electrode polarization in dielectric spectroscopy: ion mobility and mobile ion concentration of single-ion polymer electrolytes, *J. Chem. Phys. 124*, 144903.

[31] R. Casalini, and C.M. Roland [2011] On the low frequency peak in the dielectric spectrum of glycerol, *J. Chem. Phys.* **135**, 094502.

[32] R. Richert, A. Agapov, and A.P. Sokolov [2011] Appearance of a Debye peak at the conductivity relaxation frequency of a viscous liquid, *J. Chem. Phys.* **134**, 104508.

[33] G.P. Johari [2012] Electrode-spacer and other effects on the validity of the Kramers–Kronig relations and the fittings to the permittivity and electrical modulus spectra, *Thermochim. Acta* **547**, 47-52.

Table 1. Comparison of typical impedance and dielectric experiments

spectroscopy	impedance	dielectric
primary focus	electrochemical (conduction mechanisms and interfacial processes)	reorientation dynamics of molecular dipoles
sample	material-electrode system (conductive)	bulk material (capacitive)
AC voltage	$\leq 10^{-3}$ v	≤ 10 v
DC voltage	common	rare
typical analysis	equivalent circuits	relaxation models
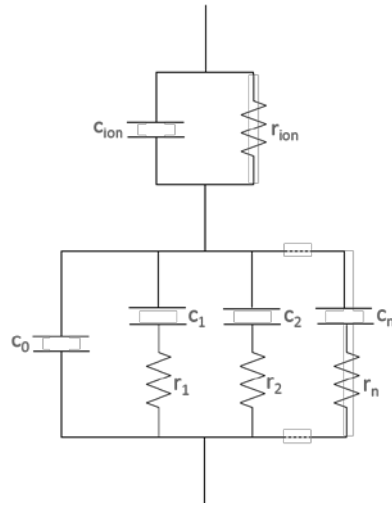
Figure 1. Equivalent circuit diagram for a viscoelastic response characterized by a distribution of *n* exponential decays, along with a contribution from mobile ions.
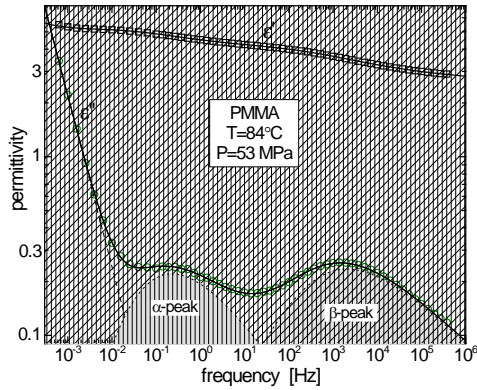
Figure 2. Dielectric spectrum of polymethylmethacrylate, along with the fits of eq. 7 and 8 to the local segmental dynamics and eq.6 for the secondary relaxation, at respective low and high frequencies. The rise in the loss below ~0.01 Hz is due to ionic conduction, fit with eq.14 using *j* = 1.
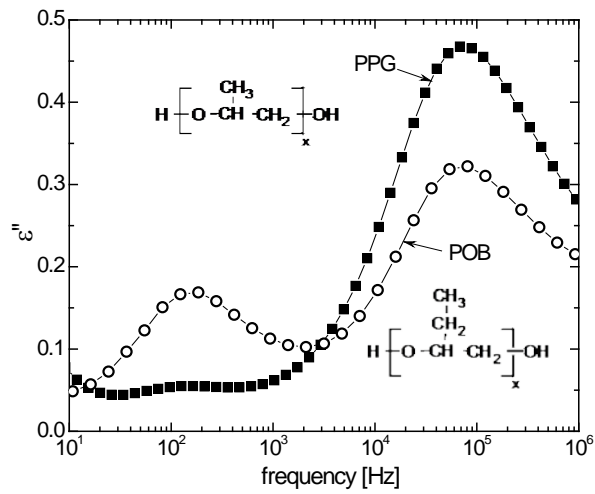
Figure 3. Dielectric loss spectra of POB and PPG having the same number of repeat units (= 67), measured at T = 20°C and P = 616 MPa (PPG) and T=24°C and P = 351 MPa (POB). The peak frequencies of the respective segmental and normal mode relaxations were 71 kHz and 143 Hz for PPG, and 99 kHz and 211 Hz for POB.
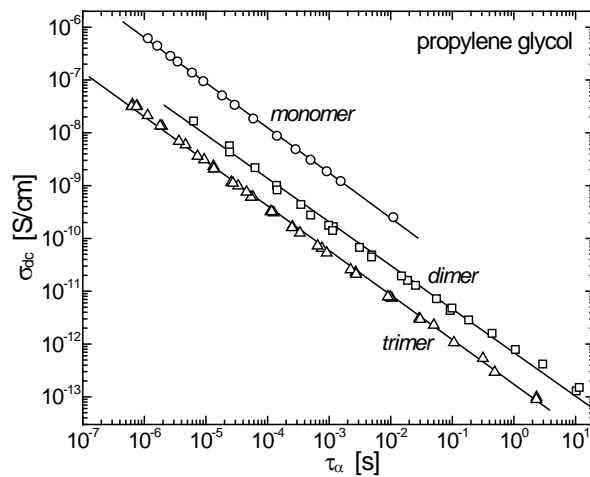
Figure 4. Conductivity vs α-relaxation time for propylene glycol monomer (circles), dimer (squares), and trimer (triangles) at various temperatures and pressures. Lines are fits yielding j=0.84±0.02 for all three liquids.
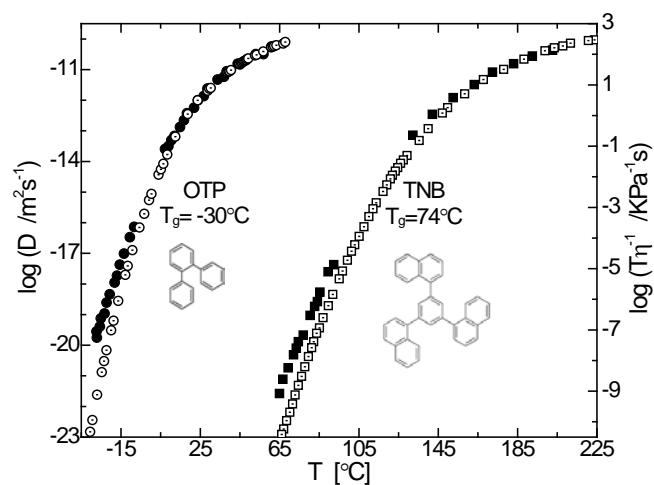
Figure 5. Self-diffusion coefficients of o-terphenyl (filled circles) and tris-naphthylbenzene (filled squares – values shifted upward by 0.16) compared to the ratio of temperature to the viscosity (corresponding open symbols). The right ordinate was adjusted to give superposition with the diffusion coefficients at high T, illustrating the enhancement of translational diffusion close to T_g. Chemical structures are shown.
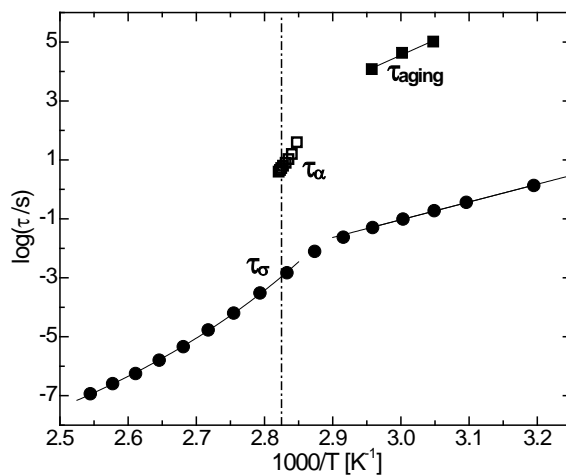

`

Figure 6. Conductivity relaxation times for carvedilol phosphate (circles), showing the weaker temperature-sensitivity below the glass transition (indicated by the vertical dashed line). Also shown (filled squares) are the time constants obtained from the change in permittivity with physical aging; these correspond to the structural relaxation time in the glass, measured directly by calorimetry near T_g (open squares).
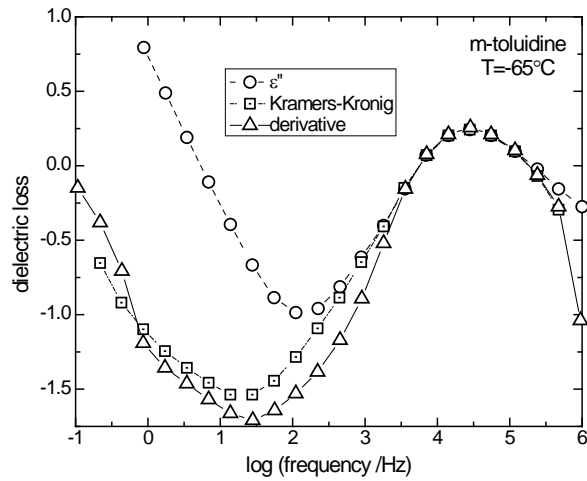
Figure 7. Dielectric loss of 3-amino toluene as measured (circles), calculated from $\varepsilon'(\omega)$ using the Kramers-Kronig relation (squares), and represented by the derivative of the real part of the permittivity. The last two methods suppress the ionic conduction, seen as the power-law at low frequencies, having a slope, -j = 1 in the present case.
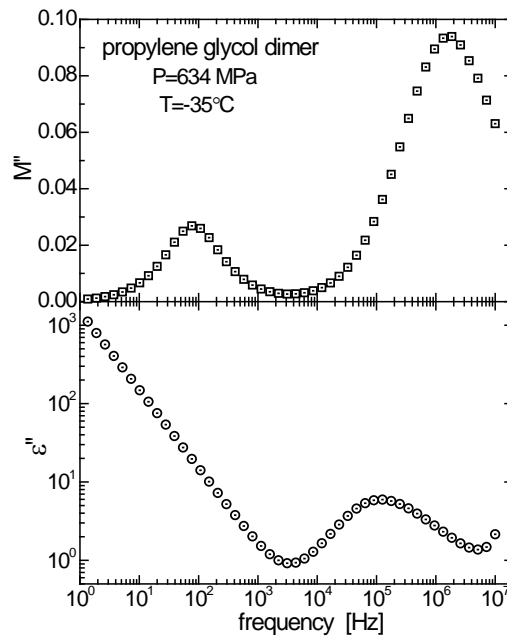

Figure 8. Imaginary component of permittivity (lower) and modulus (upper) of propylene glycol dimer. Ion conductivity is manifested in the former as a power-law at lower frequencies, and in the latter as a peak at ~10^2 Hz. Note the α-peak shifts about one decade higher frequency in the modulus representation.
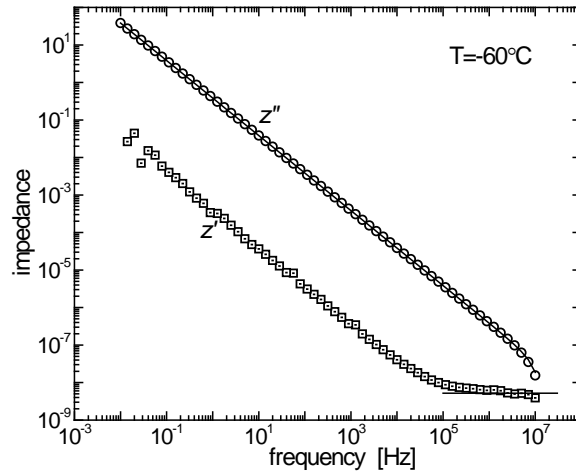
Figure 9. Real and imaginary permittivity measured for a crosslinked PVE at a temperature sufficiently low that no relaxation processes are present in the spectra. The solid lines are the fits of eq.22 to z' at high frequencies and of eq.23 to z".
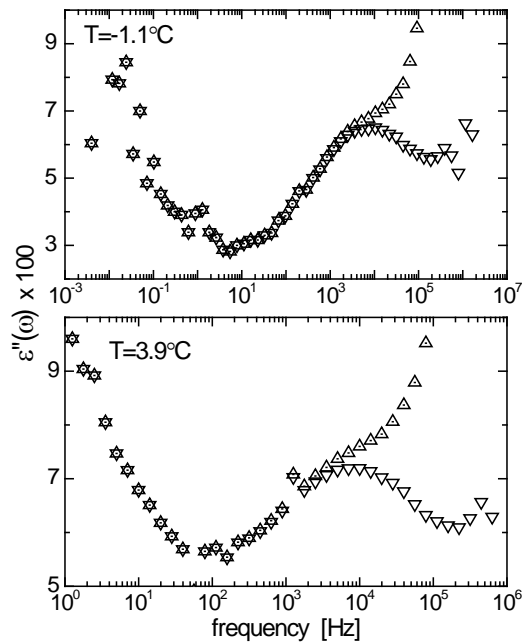

Figure 10. Dielectric loss of PVE networks at two temperatures below T_g (=9.0C). The rise at high frequencies in the measured spectra (triangles) is due to the cables; after correction (inverted triangles) the actual loss peak is obtained.
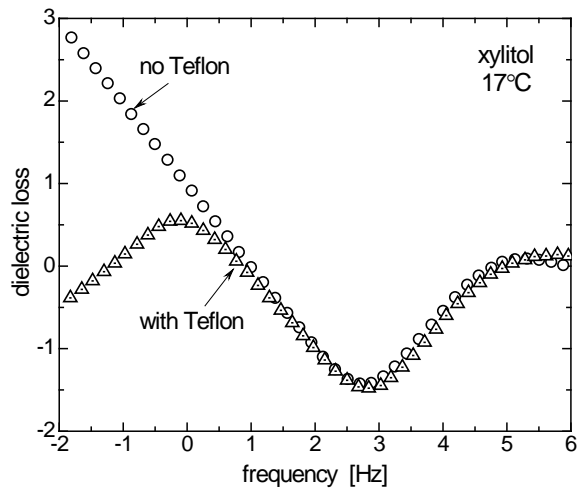
Figure 11. Dielectric loss of a polyalcohol with (triangles) and without (circles) a 5 μm Teflon film between the sample and upper electrode. The σ_{dc} manifested in a power-law at low frequencies becomes a peak around 1 Hz when the Teflon is present. The α-peak is seen at higher frequencies.
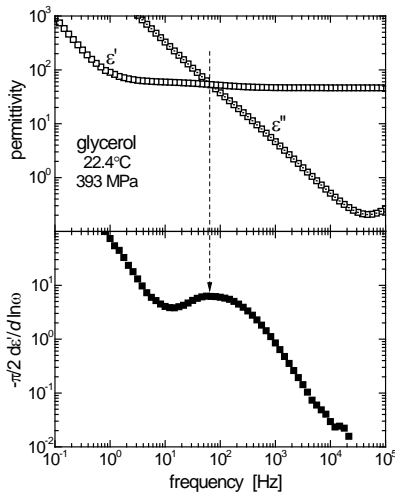

Figure 12. (top) Real (squares) and imaginary (circles) components of dielectric permittivity glycerol, showing the dominant dc-conductivity in the loss, which causes electrode polarization seen as a rise in ε' at frequencies below 1 Hz. (bottom) Derivative function (eq.19) in which σ_{dc} is manifested as a peak near the frequency at which $\varepsilon' = \varepsilon''$.